Polymers & biopolymers

Cell structure-tunable PEFT copolyester foams prepared via conducting a prior cold crystallization

Zhijun Wang[1,2], Jinggang Wang[1], Yongyan Pang[1,*] ⬤, Xinran Liu[1], Jin Zhu[1], and Wenge Zheng[1]

[1] Key Laboratory of Bio-Based Polymeric Materials Technology and Application of Zhejiang Province, Laboratory of Polymers and Composites, Ningbo Institute of Materials Technology and Engineering, Chinese Academy of Sciences, 1219 Zhongguan West Road, Ningbo 315201, Zhejiang, China

[2] Faculty of Material Metallurgical and Chemistry, Jiangxi University of Science and Technology, Ganzhou 341000, Jiangxi, China

ABSTRACT

The slow melt crystallization behavior of the new bio-based poly(ethylene terephthalate-co-ethylene 2,5-furandicarboxylate) (PEFT) copolyester makes its foaming a big challenge, thus severely hindering the exploration of its applications in the foam field. To address this issue, the objective of this study was to fabricate cell structure-tunable PEFT foams via a regulating approach of cold crystallization prior to batch foaming. First, cold crystallization via thermal annealing at a fixed temperature of 110 °C was carried out for poly(ethylene terephthalate) (PET), PEFT5%, PEFT10% and PEFT15% to investigate its effect on the foaming behavior. Second, cold crystallization at various temperatures was performed to investigate its effect on the cell structure. Third, the cell structure variation of the foams with the crystallinity was studied. Fourth, the thermal insulation of the foams was studied. It is found that with the increase in the crystallinity for all samples, the cell size decreases, the cell density increases, and the expansion ratio first increases and then decreases. Hence, the rule of cell structure variation with the crystallinity is proposed and cell structure-tunable PEFT foams are thus fabricated. In addition, microcellular PET and PEFT foams are prepared via controlling the thermal annealing temperature. Moreover, it is found that PEFT foams show comparable thermal insulation with PET foams of similar expansion ratio. Therefore, this study has made great contribution for fabricating cell structure-tunable PEFT foams and developing potential applications through improving foaming behavior via applying cold crystallization as an effective regulating approach.

Introduction

Poly(ethylene terephthalate) (PET) is a popular thermoplastic polyester, and its synthesis relies on fossil-based chemicals of ethylene glycol (EG) and terephthalic acid (PTA). PET shows good mechanical strength, dimensional stability, optical clarity and electrical insulation, and consequently has widely been applied in the fields of fibers, engineering plastics, bottles, films and foams, etc. The annual world market of PET is about 70 million tons [1–3].

Due to the gradual depletion of the non-renewable fossil-based energy, worldwide attention has been called for utilization of renewable resources for realizing sustainable development. Nature and agriculture have provided abundant bio resources, and the utilization of the waste bio resources not only reduces environmental pollution, but also produces high value added materials. Polylactic acid (PLA) is a good example of industrialization of bio-based polymers via utilizing bio-derived resources [4–7]. 2,5-furandicarboxylic acid (FDCA) is the only aromatic chemical of the twelve platform bio-based chemicals listed by the US Department of Energy for building green chemistry. As FDCA and PTA are both aromatic diacid and structurally similar, FDCA has been referred to as the ideal bio-based alternative for PTA. Hence, the new bio-based polyester synthesized with EG and FDCA, i.e., poly(ethylene 2,5-furandicarboxylate) (PEF), is regarded as the perfect bio substitute for PET [8–10]. It is noted that EG can be produced with glycerol, and FDCA can be obtained via oxidizing hydroxymethylfurfural (HMF), derived further from polysaccharides or sugars [11, 12]. Thereby, PEF can be prepared with fully bio-based chemicals. As PEF shows better mechanical strength and barrier properties than PET does [13–15], synthesis of furan-derived polyesters and copolyesters and relevant studies have become a hotspot area [16–19]. However, PEF is still much more expensive than PET, and therefore, application of poly(ethylene terephthalate-co-ethylene 2,5-furandicarboxylate) (PEFT) copolyester would be a practical route to gradually realize bio substitution for the non-renewable polyester.

The chain movement, the crystallization behavior and the physical performance of PEFT copolyesters have greatly attracted the attentions of researchers. The reported studies [20–22] show that with the increase in FDCA content, the chains become more rigid, leading to a lower melting temperature of PEFT and a slower melt crystallization rate, and the crystallization behavior of PEFT is closely related with the FDCA content. Currently, it is an important and urgent task to explore the feasible applications for the new bio-based copolyester, i.e., PEFT. However, only very limited publications [22–24] have been found focusing on potential applications of PEFT. Joshi et al. [22] and Sun et al. [23] reported that the rigid chain movement endows PEFT with better barrier properties and mechanical strength than PET. Wang et al. [24] studied the melt spinning of PEFT with FDCA content of no more than 8% to explore the feasibility for its potential application in the fiber field, and found that the properties such as the tenacity and the heat resistance of PEFT fibers achieved similar performance with that of PET fibers. Still, more application studies are urgently required toward the development of the new bio-based materials.

PET foams have wide applications in wind energy, transportation, buildings and semiconductor lighting, etc. PET shows a low melt crystallization rate as well as low melt strength, which are unfavorable for obtaining dense and small cells that are generally required by end uses [25, 26]. Various means such as chain extension [27, 28], solid-state polycondensation [29], formation of physical network [30], incorporation of nanoparticles [25] and regulation of carbon dioxide (CO_2)-induced crystallization [31, 32] have been applied to improve the foaming behavior of PET. Currently, exploration of foaming of PEFT is an important subject for opening up its potential applications in foam field. In our previous paper [33], it is found that with the increase in FDCA content, the foaming window of PEFT is gradually narrowed relative to PET, due to the decrease in both the melting temperature and sorption of CO_2 while the increase in chain rigidity. Moreover, PEFT shows even slower melt crystallization rate, leading to severe cell coalescence and collapse during foaming. Therefore, how to improve the foaming behavior of PEFT to fabricate PEFT foams with controllable cell structure is still a big challenge.

In this study, based on the crystallization behavior of PEFT, cold crystallization was applied as a regulating approach to tune the crystallization and thus the foaming behavior and the cell structure of PEFT. First, the thermal annealing of quenched PET and PEFT at a fixed temperature of 110 °C for 10 min was

carried out to study its effect on the foaming behavior. Second, the thermal annealing of quenched PET and PEFT at various temperatures for 10 min was performed to display its effect on the cell structure. Third, the effect of crystallinity on the cell structure variation of the foams was studied. Fourth, the effect of regulating cold crystallization on thermal insulation of the foams was studied.

Experimental

Materials

PET and PEFT pellets used in this study were provided by Bio-Based Polymer Materials Team of Ningbo Institute of Materials Technology and Engineering, Chinese Academy of Sciences. PET and PEFT were synthesized with the chemicals of ethylene glycol (EG), dimethyl 2,5-furandicarboxylate (DMFD) and dimethyl terephthalate (DMT) through a two-step melt polycondensation route with transesterification and subsequent polycondensation, using antimony trioxide as catalyst. The synthesis process is described in detail in the previous publication [23]. PET and PEFT prepared with the mole ratio of DMFD and DMT at 0:100, 5:95, 10:90 and 15:85 were named as PET, PEFT5%, PEFT10% and PEFT15%, respectively. Based on the results of ^{1}H NMR spectra of our previous report [33], the real FDCA content was 4.3%, 11.2%, 13.9% for PEFT5%, PEFT10% and PEFT15%, respectively. The chemical structure of PEFT copolyester is presented in Scheme 1. High-pressure carbon dioxide (CO_2) was purchased from Ningbo Wanli Gas Corporation and was used as green physical foaming agent.

Preparation of sheet samples via quenching and thermal annealing

PET and PEFT pellets were vacuum-dried at 80 °C for 12 h before use. PET and PEFT sheet samples were first prepared via quenching using compression molding, and then the samples were treated via
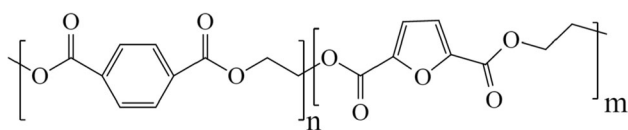
thermal annealing in an oven. PET and PEFT pellets were first melt compressed at 290 °C using a compression molding machine (XLB50-D, Huzhou Shuangli Automation Technology) under a pressure of 10 MPa for 5 min, followed by being quickly quenched into cold water. Then, the samples were thermally annealed at various temperatures in an oven (DHG-9070, Shanghai Yiheng Technology Instrument) for a fixed period of 10 min. It is noted that PET and PEFT sheets prepared via quenching without thermal annealing were used for the purpose of comparison. All the sheet samples had a diameter of 25 mm and a thickness of 1 mm and were used in the following experiments.

Characterization of crystallization

Characterization of crystallization of samples prepared via quenching and thermal annealing with DSC

A differential scanning calorimeter (DSC) (TGA/DSC1, Mettler Toledo) was used to study the crystallization of PET and PEFT sheets prepared via quenching and thermal annealing at various temperatures for 10 min using compression molding. The sample of 5–10 mg was heated directly from 30 °C to 300 °C at 10 °C/min under N_2 atmosphere, and the heating curves were recorded. The crystallinity (X_c) of PET and PEFT prepared via quenching and thermal annealing is calculated according to Eq. 1 [32].

$$\chi_c = \frac{\Delta H_m - \Delta H_{cc}}{\Delta H_{m0}} \tag{1}$$

where ΔH_m is the enthalpy of fusion, ΔH_{cc} is the enthalpy of cold crystallization. ΔH_{m0} is the enthalpy of fusion of 100% crystalline polymer, and is 140 J/g for PET [21, 30].

In addition, the isothermal cold crystallization of quenched PET and PEFT was also studied with DSC. The sample was heated from 30 to 110 °C at the rate of 100 °C/min, and then was kept at 110 °C for 60 min, and the isothermal cold crystallization curves were recorded.

Characterization of crystallization of samples prepared via quenching and thermal annealing with WAXD

The crystallization of PET and PEFT sheets prepared via quenching and thermal annealing at various

Scheme 1 Chemical structure of PEFT.

temperatures was also studied with wide angle X-ray diffraction (WAXD) using an X-ray diffractometer (D8 Advance Davinci, Bruker) with CuKα radiation (λ = 0.154 nm) operating at 40 kV. The data scan was collected in 2θ angle range of 5°–60° for 10 min.

Effect of thermal annealing on CO_2 sorption

The sorption of CO_2 in PET and PEFT prepared via quenching and thermal annealing at various temperatures was conducted with a high-pressure vessel. First, the sheet samples were put in the vessel, which was pressurized with CO_2 to a saturation pressure of 4 MPa at room temperature. Second, after saturation of 72 h, the pressure inside the vessel was released, and the sheet samples were quickly transferred to a digital balance to measure the sample weight. Third, the amount of CO_2 absorbed in the sheet samples is calculated based on Eq. 2 [32].

$$M_t = (m_t - m_0)/m_0 \tag{2}$$

where M_t is the amount of CO_2 absorbed in the polymer matrix, m_0 and m_t are the weight of the samples before and after saturation in CO_2 atmosphere, respectively.

Batch foaming and cell structure observation

It is known that the batch foaming approach is favorable for investigating the effect of the precedent phase morphology on the cell structure [34–36]. Hence, batch foaming was applied in the present work to study the effect of thermal annealing on the cell structure of PET and PEFT foams. First, the sample sheets prepared via quenching and thermal annealing were put in a high-pressure vessel at room temperature. Then, after being flushed with a small amount of CO_2 to vent the air, the vessel was pressurized to 4 MPa for the samples to be saturated at room temperature for 72 h. Next, following a rapid release of the pressure at the end of the saturation process, the sample sheets were quickly transferred from the vessel to a dimethyl silicone bath set at 180 °C to foam for 20 s. Finally, PET and PEFT foam samples were immediately immersed into cold water to solidify the cell structure.

The cell structure of PET and PEFT foams was studied using a scanning electron microscope (SEM) (EVO18, Zeiss) at an acceleration voltage of 20 kV.

The foams were freeze-fractured after immersing in liquid nitrogen for 10 min, and then were sputter-coated with a layer of Pt on the fractured surface for SEM characterization.

The mass density of the solid (ρ_0) and the foam (ρ_f) samples was measured using an analytical balance according to the water displacement method based on the standard of ASTM D792-07. The expansion ratio (R_v) of PET and PEFT foams is calculated according to Eq. 3 [37].

$$R_v = \frac{\rho_0}{\rho_f} \tag{3}$$

The cell size and the cell density of PET and PEFT foams were measured and calculated with the Image-Pro Plus software. The diameter of at least 200 cells was measured to calculate the average cell size, and the cell density (N_n) is calculated using Eq. 4 [38].

$$N_n = \left(\frac{n}{A}\right)^{3/2} \times R_v \tag{4}$$

where n is the cell number in the SEM micrograph, and A is the area of the micrograph (cm^2).

Thermal conductivity measurement

A laser thermal conductivity analyzer (LFA 467, NETZSCH) was employed to measure the thermal conductivity of PET and PEFT foams. The foams were cut into the small squared piece with the length and the width both of 10 mm, and subsequently, the surface of each piece was uniformly sprayed with a layer of graphite. The thermal insulation of each sample was measured five times under the same condition at 25 °C, and the average thermal conductivity was presented.

Results and discussion

Exploring effect of cold crystallization on foaming behavior

Regulating cold crystallization via thermal annealing at a fixed temperature

The DSC heating curves of PET, PEFT5%, PEFT10% and PEFT15% prepared via quenching are shown in Fig. 1a₁, and the related parameters are presented in Table 1. With the increase in FDCA content, the cold crystallization temperature of PEFT increases, and
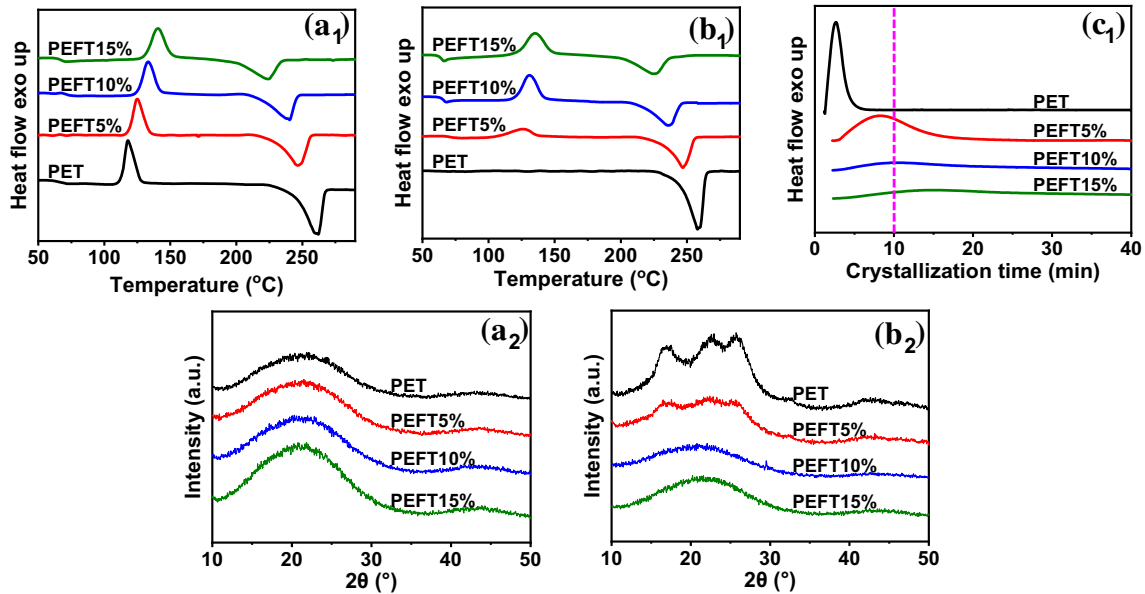
Figure 1 a_1, b_1 DSC heating curves and a_2, b_2 WAXD intensity curves of PET and PEFT prepared via a_1, a_2 quenching and b_1, b_2 thermal annealing at 110 °C for 10 min. c_1 DSC isothermal cold crystallization curves of samples prepared via quenching during thermal annealing at 110 °C, with a pink dashed line to clearly indicate the degree to which the cold crystallization proceeded within 10 min.

Table 1 Thermal properties of PET and PEFT prepared via quenching and thermal annealing at 110 °C for 10 min

Sample	T_{cc} (°C)	T_m (°C)	ΔH_{cc} (J/g)	ΔH_m (J/g)	χ_c (%)
PET	119.3	258.4	53.2	74.7	15.3
PEFT5%	125.6	246.2	32.8	47.1	10.2
PEFT10%	133.0	240.3	29.8	36.4	4.7
PEFT15%	142.6	224.2	28.0	28.8	0.6
PET/110 °C	–	258.3	–	76.8	54.8
PEFT5%/110 °C	124.7	247.3	4.4	49.8	32.4
PEFT10%/110 °C	130.6	239.6	20.7	37.1	11.7
PEFT15%/110 °C	137.3	224.4	25.4	29.2	2.7

the melting temperature and the crystallinity decrease (Fig. 1a$_1$; Table 1). Cold crystallization is actually a crystallization phenomenon that happens during the post heating scan generally for polymers such as PLA and PET that have an intrinsic slow melt crystallization rate [5, 6, 25, 39]. Cold crystallization is usually used to evaluate the precedent melt crystallization ability or kinetics of semi-crystalline polymers. A higher cold crystallization temperature generally means that the precedent melt crystallization is more difficult to happen, or it proceeds only to a lower degree within a limited time period. In this study, with the increase in FDCA content, the decreased melting temperature and crystallinity of

PEFT were attributed to the more hindered chain movement, hence leading to the more difficult occurrence of melt crystallization and thus the formation of crystals of lower perfection, which further led to cold crystallization occurring at higher temperatures during the post heating scan. Similar observation was also reported in the previous study [21]. It is noted here that the crystallinity for quenched PET, PEFT5%, PEFT10% and PEFT15% was 15.3%, 10.2%, 4.7% and 0.6%, respectively, meaning that weak melt crystallization still happened during the quenching (Table 1).

The DSC heating curves in Fig. 1a$_1$ show that the onset cold crystallization temperature was 110.2, 115.3, 122.6 and 128.4 °C for the quenched samples of PET, PEFT5%, PEFT10% and PEFT15%, respectively. Based on the result, 110 °C was chosen as a fixed annealing temperature to explore the effect of cold crystallization on the foaming behavior of PET and PEFT copolyesters. The DSC heating curves of PET, PEFT5%, PEFT10% and PEFT15% prepared via thermal annealing at 110 °C for 10 min are shown in Fig. 1b$_1$. Two changes about the cold crystallization were observed after thermal annealing (Fig. 1b$_1$; Table 1). First, the cold crystallization peak disappeared for PET, and the enthalpy of cold crystallization was significantly reduced for PEFT5%,

followed by PEFT10% and PEFT15% in a decreasing order. The cold crystallization temperature of PEFT5%, PEFT10% and PEFT15% all decreased relative to those of the quenched counterparts. These phenomena were attributed to the fact that cold crystallization could occur during both the precedent thermal annealing and the post heating scan. If it had already proceeded to some degree during the precedent process but had not yet finished, its further occurrence during the post heating might require less energy. Second, the crystallinity of the samples all increased after thermal annealing, with PET gaining the largest, followed by PEFT5%, PEFT10% and PEFT15%.

The isothermal cold crystallization curves of quenched PET and PEFT during the thermal annealing at 110 °C are presented in Fig. $1c_1$. It can be seen that the cold crystallization finished within 10 min for PET, finished more than half for PEFT5%, and partially finished for PEFT10% and PEFT15%. This suggests that with the increase in FDCA content, the cold crystallization of PEFT turned much slower. Our previous study [20] as well as those by Konstantopoulou et al. [21] and Joshi et al. [22] also showed that the increase in FDCA content led to the slower melt crystallization rate of PEFT. Hence, it is quite clear that the incorporation of FDCA hinders both the melt crystallization and the cold crystallization. Thereby, the results of Fig. $1c_1$ provided a solid interpretation for quenched PEFT with a higher FDCA content which gained a lower crystallinity after thermal annealing within 10 min (Fig. $1b_1$).

The WAXD intensity curves of PET, PEFT5%, PEFT10% and PEFT15% prepared via quenching and thermal annealing at 110 °C for 10 min are shown in Figs. $1a_2$ and $1b_2$, respectively. All the quenched samples did not show crystalline patterns, probably due to the fact that the low crystallinity formed during quenching might hardly be detected by WAXD (Fig. $1a_2$). However, it can be observed that the amorphous halo was lower for PEFT with lower content of FDCA. After thermal annealing, the amorphous halo decreased in area for all samples. PET showed characteristic peaks located at 16.7°, 22.4° and 25.6°, consistent with the previous report [40]. PEFT5% showed weak diffraction peaks at the similar positions, while PEFT10% and PEFT15% did not show any characteristic peaks (Fig. $1b_2$). The results indicated again that the increase in FDCA content led to the occurrence of cold crystallization of

PEFT more difficult. Hence, the different crystallization ability of PEFT made it possible that the crystallization of the samples can be tuned to different degrees via cold crystallization at a fixed annealing temperature for the same time period, which is proved by the results of Fig. 1.

Effect of regulating cold crystallization on foaming behavior

The cell structure of PET and PEFT foams was studied to explore the effect of regulating cold crystallization on foaming behavior. The cell structure of PET, PEFT5%, PEFT10% and PEFT15% foams prepared via quenching and thermal annealing at 110 °C for 10 min is showed in Fig. 2. Four different phenomena were observed through comparing the cell structure of the four samples prepared via quenching and thermal annealing. For quenched PET, uniform cell structure was observed, while the sample was not able to foam after thermal annealing. This was attributed to the too large crystallinity formed during the thermal annealing, which suppressed both the cell nucleation due to the decrease in the CO_2 sorption and the cell growth [41, 42]. For quenched PEFT5%, big cells were observed, while dense and small cells were formed after thermal annealing. This is attributed to the relatively large crystallinity facilitating the heterogeneous cell nucleation but suppressing the cell growth [31, 43]. For quenched PEFT10%, severe cell coalescence was observed, and in comparison, uniform cells were formed after thermal annealing. This is attributed to the proper crystallinity formed in the sample favoring both the heterogeneous cell nucleation and the cell growth [30]. For quenched PEFT15%, severe cell collapse was observed, and only slight improvement of the cell structure was observed after thermal annealing. This is attributed to the too low crystallinity formed during the thermal annealing, which did not show significant effect on improvement of the melt strength.

The expansion ratio of PET and PEFT foams prepared via quenching and thermal annealing at 110 °C for 10 min is presented in Fig. 3. The striking contrast was observed for PET, as PET after annealing was hardly foamed, and its expansion ratio was only about 1. Compared to that of the quenched counterpart, the expansion ratio after annealing was significantly decreased for PEFT5%, while obviously increased for PEFT10%, and a slight increase was

Figure 2 Cell structure of PET and PEFT foams prepared via quenching and thermal annealing at 110 °C and then foaming at 180 °C.
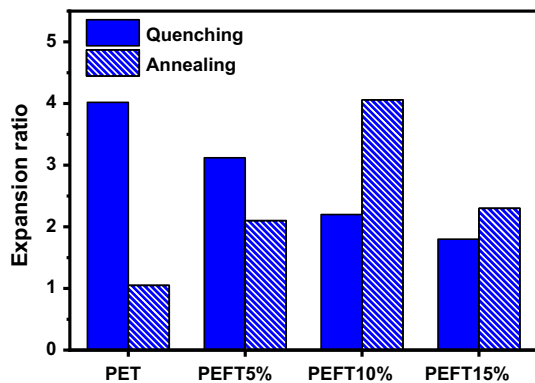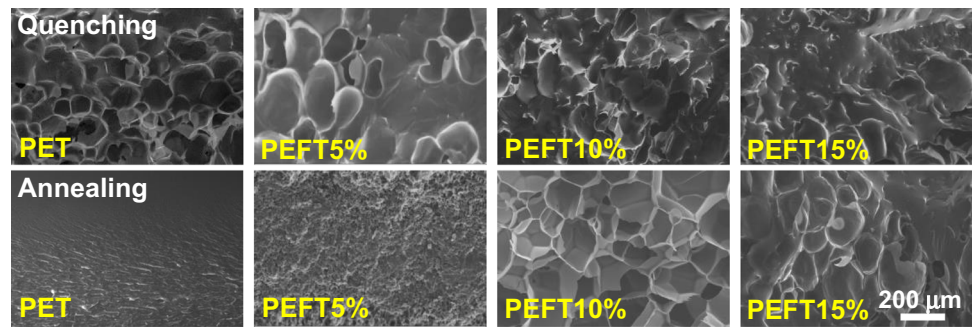

Figure 3 Expansion ratio of PET and PEFT foams prepared via quenching and thermal annealing at 110 °C and then foaming at 180 °C.

observed for PEFT15%. The change of the expansion ratio after thermal annealing agreed well with that of the cell structure. The results indicated that the crystallinity gained during the thermal annealing really plays a significant role in affecting the foaming behavior, consistent with the previous study about foaming of low density polyethylene with a series of preset crystallinity [42]. Further, as the cold crystallization rate was much slower for PEFT with higher content of FDCA, it is hence considered that higher thermal annealing temperatures would be required for more effectively regulating the cold crystallization of those PEFT and thus favorable for exploring the effect of the crystallization on the cell structure variation for all samples.

Revealing effect of cold crystallization on cell structure

Regulating cold crystallization via thermal annealing at various temperatures

The DSC heating curves of PET and PEFT10% prepared via quenching and thermal annealing at various temperatures for a fixed time period of 10 min is shown in Fig. 4a_1 and b_1. Two series of various thermal annealing temperatures were set for conducting cold crystallization, one series for PET and PEFT5%, and the other series for PEFT10% and PEFT15%. With the increase in the thermal annealing temperature, the cold crystallization temperature gradually moved to lower temperature direction, and the cold crystallization peak became gradually weaker or even disappeared. The results were attributed to the fact that cold crystallization occurred during the thermal annealing. The higher the thermal annealing temperature was, and the larger degree the cold crystallization had already proceeded. Hence, it became weaker during the post heating scan. The previous studies [44, 45] also showed that the cold crystallization of PLA proceeded faster at higher isothermal temperatures. The WAXD intensity curves of PET and PEFT10% prepared via quenching and thermal annealing at various temperatures for 10 min is shown in Fig. 4a_2 and b_2. With the increase in the annealing temperature, the amorphous halo gradually decreased, and the crystalline characteristic peaks gradually appeared and increased in intensity. The results of WAXD were consistent with the results of DSC above.

The crystallinity of PET, PEFT5%, PEFT10% and PEFT15% as a function of the annealing temperature is shown in Fig. 5a. With the increase in the thermal annealing temperature, the crystallinity increased for all samples, indicating that regulating the cold crystallization via thermal annealing was effective in tuning the crystallinity. The mass uptake of CO_2 in PET, PEFT5%, PEFT10% and PEFT15% after annealing at various temperatures for 10 min is shown in Fig. 5b. With the increase in the annealing temperature, the mass uptake of CO_2 decreased for all samples, attributed to the higher crystallinity suppressing the sorption of CO_2 [41].

Figure 4 a_1, b_1 DSC heating curves and a_2, b_2 WAXD intensity curves of a_1, a_2 PET and b_1, b_2 PEFT10% prepared via quenching and thermal annealing at various temperatures for 10 min.
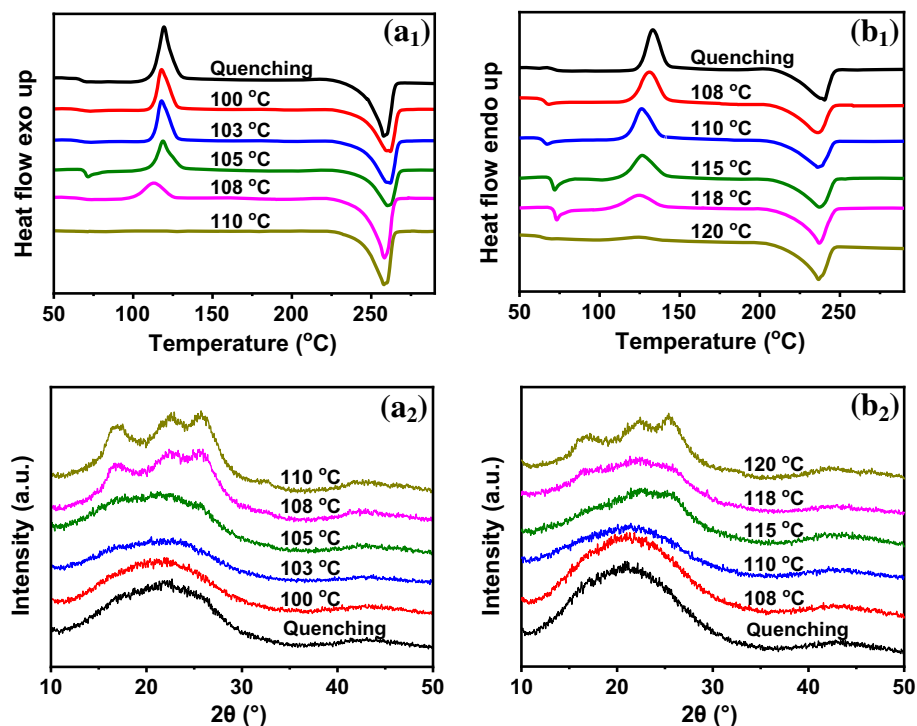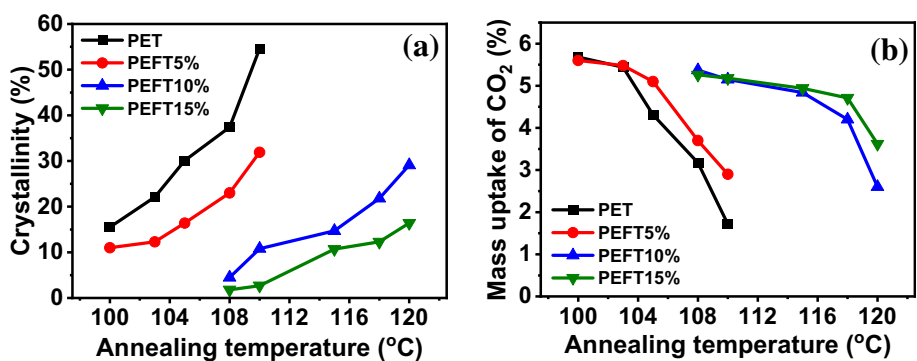

Figure 5 **a** Crystallinity and **b** mass uptake of CO_2 of PET and PEFT as a function of the thermal annealing temperature.

Effect of cold crystallization on cell structure

The cell structure of PET, PEFT5%, PEFT10% and PEFT15% foams prepared via quenching and thermal annealing at various temperatures for 10 min is shown in Fig. 6. Generally, with the increase in the annealing temperature for all samples, the phenomenon of cell coalescence gradually disappeared, and the cell size gradually became smaller, and some samples turned not even able to foam. These results were attributed to the gradual increase in the crystallinity, which affected both the heterogeneous cell nucleation and the cell growth [42, 43]. In specific, for PEFT with a higher FDCA content, a higher low-end thermal annealing temperature was required for cell coalescence to disappear, and in parallel, the sample

became not able to foam also at a higher high-end thermal annealing temperature. Hence, the results proved that higher annealing temperatures were required for PEFT with a higher content of FDCA to conduct cold crystallization of 10 min for effectively improving the cell structure, ascribed to its slow crystallization rate. In addition, for PET foam prepared via thermal annealing at 108 °C, the cell size was about 2.2 μm. For PEFT5% foam via annealing at 110 °C, the cell size was about 2.4 μm. Hence, PET and PEFT5% foams with cells in micro size were fabricated via regulating cold crystallization.

The cell size, cell density and expansion ratio of PET, PEFT5%, PEFT10% and PEFT15% foams as a function of the thermal annealing temperature are shown in Fig. 7. It can be seen that with the increase
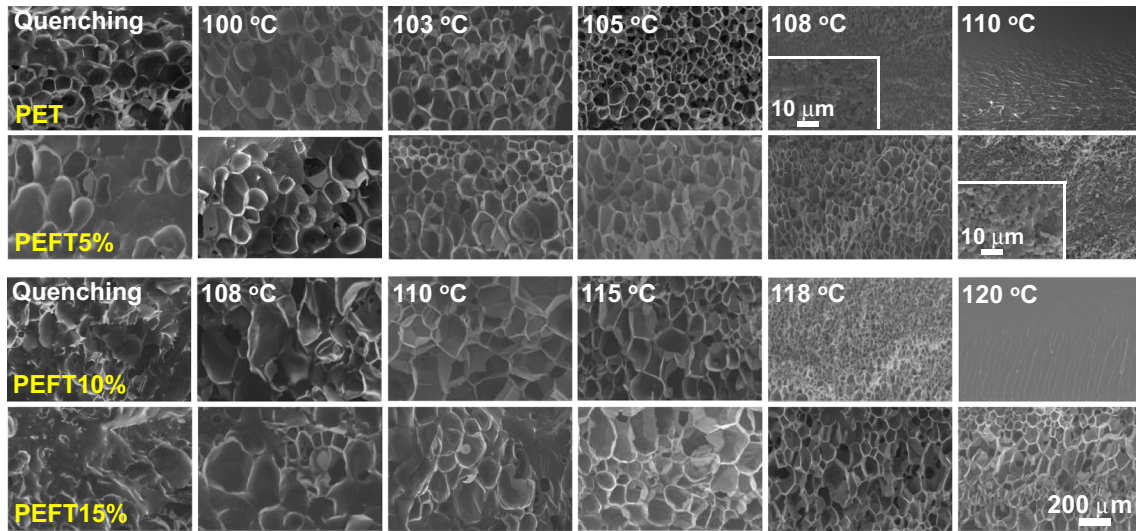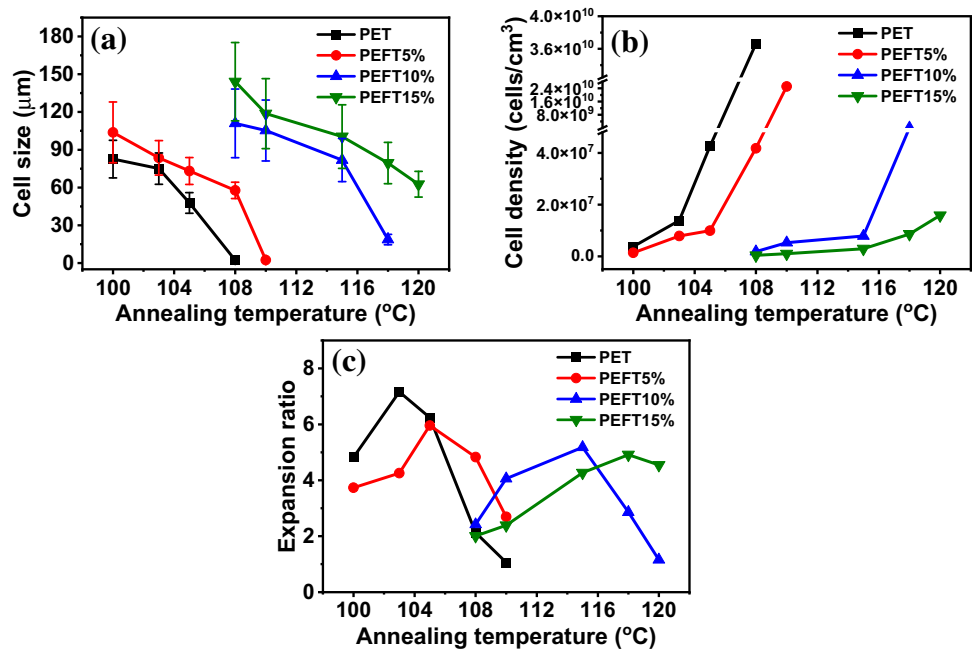
Figure 6 Cell structure of PET and PEFT foams prepared via quenching and thermal annealing at various temperatures for 10 min and then foaming at 180 °C.

Figure 7 Cell structure change of PET and PEFT foams with the thermal annealing temperature: **a** cell size, **b** cell density and **c** expansion ratio.

in the thermal annealing temperature, the cell size all decreased (Fig. 7a), the cell density all increased (Fig. 7b), and the expansion ratio all first increased and then decreased (Fig. 7c). The results were attributed to the increase in the crystallinity, which brings increase in heterogeneous cell nucleation, decrease in sorption of CO_2, and increase in stiffness of polymer matrix [41–43]. The previous studies reported that the cell structure of PLA foams can also

be tuned via controlling the crystallization through incorporating heterogeneous nucleating agent [46], adjusting the crystal type [47] and controlling the crystalline structure [48, 49], etc. In Fig. 7c, it can be seen that an optimum thermal annealing temperature existed for each sample, where the expansion ratio was the maximum. With the increase in FDCA content, the optimum annealing temperature of PEFT increased. It appeared that a higher annealing

temperature was required for PEFT with a slower crystallization rate. In addition, it has already been discussed that PET and PEFT5% foams with micro-sized cells were fabricated (Fig. 6). Figure 7a shows that with the increase in the thermal annealing temperature, the cell size decreased from about 100 μm to about 2 μm. Figure 7b shows that with the increase in the annealing temperature from 100 to 108 °C, the cell density of PET foam increased from 3.76×10^6 to 3.66×10^{10} cells/cm^3, and from 100–110 °C, the cell density of PEFT5% foam increased from 1.38×10^6 to 2.52×10^{10} cells/cm^3. Therefore, this study has provided solid evidence that cold crystallization can be applied as an effective approach for tuning microcellular PET and PEFT foams.

Studying effect of crystallinity on cell structure variation

The cell size, cell density and expansion ratio of PET, PEFT5%, PEFT10% and PEFT15% foams versus the crystallinity is shown in Fig. 8. The cell size, cell density and expansion ratio of the quenched samples were also presented for comparison, at the lowest crystallinity for each line. With the increase in the crystallinity, the cell size all decreased (Fig. 8a), the cell density all increased (Fig. 8b), and the expansion ratio all first increased and then decreased (Fig. 8c). In Fig. 8c, it can be seen that an optimum crystallinity existed for each sample, where the value of the expansion ratio reached the maximum. With the increase in the FDCA content, the optimum crystallinity of PEFT decreased, ascribed to its low crystallization ability. In addition, it is considered that when the crystallinity increases from a very low value to the optimum, the enhancement of heterogeneous cell nucleation plays the leading role in determining the change of the cell structure in the trend that the cell size decreases, the cell density increases and the expansion ratio increases. When the crystallinity further increases from the optimum to even larger, the increase in stiffness of polymer matrix and decrease in CO_2 sorption together play the dominant role in deciding the change of the cell structure in another trend that the cell size decreases, the cell density increases and the expansion ratio decreases. Hence, the rule of the cell structure variation with the crystallinity is proposed in this study. In a previous review article [50], we found that the cell structure variation of polymer nanocomposite foams with the content of nanoparticle follows the similar rule. The details of the effect of the nanoparticle content on the cell structure variation can be found in the published literature [51, 52]. Hence, it is understandable that the crystal plays a similar role as the nanoparticle does in tuning the cell structure of polymer foams. Based on this, cell structure-tunable PEFT foams are fabricated via applying cold crystallization as the regulating approach without incorporating nanoparticles.

Figure 8 Cell structure variation of PET and PEFT foams with the crystallinity: **a** cell size, **b** cell density and **c** expansion ratio. The cell size, cell density and expansion ratio of samples prepared via quenching are also presented at the lowest crystallinity for comparison.
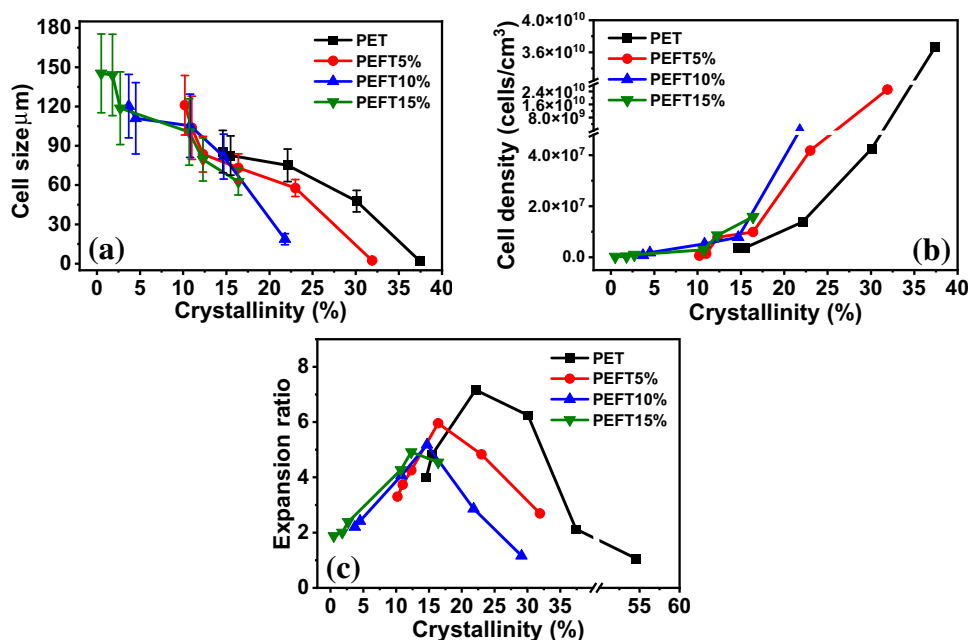
Showing the effectiveness of regulating cold crystallization on thermal insulation

The thermal insulation of PEFT foams was studied to explore the potential applications for the new bio-based material. The thermal insulation of PET, PEFT5%, PEFT10% foams was studied to show the effectiveness of regulation of cold crystallization on the physical performance. The thermal conductivity of PEFT10% foams as a function of the thermal annealing temperature is shown in Fig. 9a. First, the thermal conductivity decreased for the foam prepared at the annealing temperature from 108 to 115 °C, and then increased to the foam annealing at 118 °C, and further increased to the foam at 120 °C. The lowest thermal conductivity was observed for the foam annealing at 115 °C. It was found that the change trend of the thermal conductivity was reversely related with that of the expansion ratio (Fig. 7c). This was ascribed to the thermal conductivity of the air being much lower compared to that of the polymer matrix [53–55]. Second, the thermal conductivity of PEFT10% foams prepared with thermal annealing at 108, 110, 115 and 118 °C was all smaller than that of the quenched counterpart. This proved the effectiveness of the cold crystallization to tune the cell structure and thus the thermal insulation. Third, the thermal conductivity of PEFT10% foam prepared with thermal annealing at 120 °C was similar as that of the unfoamed PEFT10% sheet. This was due to the fact that a too high thermal annealing temperature generated a too high crystallinity, which led to the sample hardly foaming. The thermal conductivity of PET, PEFT5% and PEFT10% foams as a function of

the expansion ratio is shown in Fig. 9b. First, with the increase in the expansion ratio, the thermal conductivity decreased for all samples, consistent with other polymer foams [4, 5]. Second, the thermal conductivity of PEFT foams was comparable with that of PET foams of similar expansion ratio, indicating that PEFT foam would be a good substitute for PET foam in the area concerning thermal insulation.

Conclusions

In this study, cold crystallization via thermal annealing was applied as a regulating approach to tune the crystallization of PEFT prior to batch foaming and thus to fabricate cell structure-tunable PEFT foams. First, cold crystallization via thermal annealing at 110 °C was performed for PET, PEFT5%, PEFT10% and PEFT15% to investigate its effect on the foaming behavior. It is found that cold crystallization at 110 °C showed four different effects on the foaming behavior of the four samples. Second, cold crystallization via thermal annealing at various temperatures were carried out for four samples to investigate its effect on the cell structure. It is found that with increase in the thermal annealing temperature for all sheet samples, the crystallinity increases while the sorption of CO_2 decreases. For the foam samples, the cell size all decrease, the cell density all increase, and the expansion ratio all first increase and then decrease. Based on this, microcellular PET and PEFT5% foams are prepared via applying thermal annealing at 108 and 110 °C, respectively. Third, the effect of the crystallinity on the cell structure
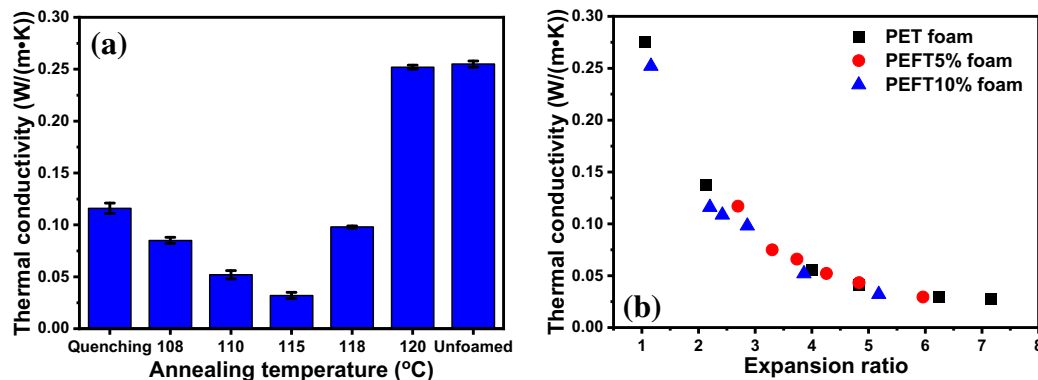

Figure 9 a Thermal conductivity of PEFT10% foams as a function of the annealing temperature. Thermal conductivity of PEFT10% foam prepared via quenching and unfoamed sheet are also presented for comparison. **b** Thermal conductivity of PET, PEFT5% and PEFT10% foams as a function of the expansion ratio.

variation of the foams was studied. It is found that the cell structure variation with the crystallinity for all samples shows the same change trend, similar as that with the thermal annealing temperature. Hence, the rule of cell structure variation with the crystallinity is proposed, and based on this, cell structure-tunable PEFT foams are thus fabricated. Fourth, the effect of cold crystallization via thermal annealing on thermal insulation of PET and PEFT foams was studied. It is found that PEFT foams show comparable thermal conductivity with PET foams of similar expansion ratio, indicating that PEFT foams would be good bio-based substitute for PET foams in the thermal insulation aspect. Therefore, this study has provided an effective approach via regulating cold crystallization to fabricate cell structure-tunable PEFT foams, which is of great importance for opening up the potential applications of the new bio-based foams.

Acknowledgments

Declarations

Conflict of interest The authors declare that they have no known competing financial interests or personal relationships that could have appeared to influence the work reported in this paper.

References

[1] Girard M, Combeaud C, Billon N (2021) Effects of annealing prior to stretching on strain induced crystallization of polyethylene terephthalate. Polymer 230:124078

[2] Zhang X, Zhao SC, Mohamed MG, Kuo SW, Xin Z (2020) Crystallization behaviors of poly(ethylene terephthalate) (PET) with monosilane isobutyl-polyhedral oligomeric silsesquioxanes (POSS). J Mater Sci 55:14642–14655 https://doi.org/10.1007/s10853-020-05003-9

[3] Yao S, Guo T, Liu T, Xi Z, Xu Z, Zhao L (2020) Good extrusion foaming performance of long-chain branched PET induced by its enhanced crystallization property. J Appl Polym Sci 137:49268

[4] Wang G, Zhao J, Wang G, Zhao H, Lin J, Zhao G, Park CB (2020) Strong and super thermally insulating in-situ nanofibrillar PLA/PET composite foam fabricated by high-pressure microcellular injection molding. Chem Eng J 390:124520

[5] Wang J, Chai J, Wang G, Zhao J, Zhang D, Li B, Zhao H, Zhao G (2019) Strong and thermally insulating polylactic acid/glass fiber composite foam fabricated by supercritical carbon dioxide foaming. Int J Biol Macromol 138:144–155

[6] Li Y, Yin D, Liu W, Zhou H, Zhang Y, Wang X (2020) Fabrication of biodegradable poly(lactic acid)/carbon nanotube nanocomposite foams: Significant improvement on rheological property and foamability. Int J Biol Macromol 163:1175–1186

[7] Kuang T, Ju J, Chen F, Liu X, Zhang S, Liu T, Peng X (2022) Coupled effect of self-assembled nucleating agent, Ni-CNTs and pressure-driven flow on the electrical, electromagnetic interference shielding and thermal conductive properties of poly (lactic acid) composite foams. Compos Sci Technol 230:109736

[8] Knoop RJI, Vogelzang W, van Haveren J, van Es DS (2013) High molecular weight poly(ethylene-2,5-furanoate); critical aspects in synthesis and mechanical property determination. J Polym Sci Pol Chem 51:4191–4199

[9] Sousa AF, Vilela C, Fonseca AC, Matos M, Freire CSR, Gruter GJM, Coelhob JFJ, Silvestrea AJD (2015) Biobased polyesters and other polymers from 2,5-furandicarboxylic acid: a tribute to furan excellency. Poly Chem 6:5961–5983

[10] Fei X, Wang J, Zhu J, Wang X, Liu X (2020) Biobased poly(ethylene 2,5-furancoate): no Longer an alternative, but an irreplaceable polyester in the polymer industry. ACS Sustain Chem Eng 8:8471–8485

[11] Gandini A, Silvestre AJD, Neto CP, Sousa AF, Gomes M (2009) The furan counterpart of poly(ethylene terephthalate): an alternative material based on renewable resources. J Polym Sci Pol Chem 47:295–298

[12] Gomes M, Gandini A, Silvestre AJD, Reis B (2011) Synthesis and characterization of poly(2,5-furan dicarboxylate)s based on a variety of diols. J Polym Sci Pol Chem 49:3759–3768

[13] Burgess SK, Leisen JE, Kraftschik BE, Mubarak CR, Kriegel RM, Koros WJ (2014) Chain mobility, thermal, and mechanical properties of poly(ethylene furanoate) compared to poly(ethylene terephthalate). Macromolecules 47:1383–1391

[14] Burgess SK, Karvan O, Johnson JR, Kriegel RM, Koros WJ (2014) Oxygen sorption and transport in amorphous poly(ethylene furanoate). Polymer 55:4748–4756

[15] Burgess SK, Kriegel RM, Koros WJ (2015) Carbon dioxide sorption and transport in amorphous poly(ethylene furanoate). Macromolecules 48:2184–2193

[16] Zhang H, Jiang M, Wu Y, Li L, Wang Z, Wang R, Zhou G (2021) Development of completely furfural-based renewable polyesters with controllable properties. Green Chem 23:2437–2448

[17] Zhou G, Li L, Jiang M, Wang G, Wang R, Wu G, Zhou G (2021) Renewable poly(butene 2,5-furan dicarboxylate) nanocomposites constructed by TiO_2 nanocubes: synthesis, crystallization, and properties. Polym Degrad Stabil 189:109591

[18] Wang J, Liu X, Zhang Y, Liu F, Zhu J (2016) Modification of poly(ethylene 2,5-furandicarboxylate) with 1,4-cyclohexanedimethylene: influence of composition on mechanical and barrier properties. Polymer 103:1–8

[19] Shen A, Wang G, Wang J, Zhang X, Fei X, Fan L, Zhu J, Liu X (2021) Poly(1,4-butylene-co-1,4-cyclohexanedimethylene 2,5-furandicarboxylate) copolyester: potential bio-based engineering plastic. Eur Polym J 147:110317

[20] Wang Z, Wang J, Pang Y, Zhu J, Zheng W (2022) Comparing non-isothermal melt and cold crystallization behavior and kinetics of poly(ethylene 2,5-furandicarboxylate-co-ethylene terephthalate) copolyesters. J Mater Sci 57:17503–17516 https://doi.org/10.1007/s10853-022-07710-x

[21] Konstantopoulou M, Terzopoulou Z, Nerantzaki M, Tsagkalias J, Achiliasb DS, Bikiaris DN, Exarhopoulos S, Papageorgiou DG, Papageorgiou GZ (2017) Poly(ethylene furanoate-co-ethylene terephthalate) biobased copolymers: synthesis, thermal properties and cocrystallization behavior. Eur Polym J 89:349–366

[22] Joshi AS, Lawrence JG, Coleman MR (2019) Effect of biaxial orientation on microstructure and properties of renewable copolyesters of poly(ethylene terephthalate) with 2,5-furandicarboxylic acid for packaging application. ACS Appl Polym Mater 1:1798–1810

[23] Sun L, Zhang Y, Wang J, Liu F, Jia Z, Liu X, Zhu J (2019) 2,5-Furandicarboxylic acid as a sustainable alternative to isophthalic acid for synthesis of amorphous poly(ethylene terephthalate) copolyester with enhanced performance. J Appl Polym Sci 136:47186

[24] Wang P, Huang W, Zhang Y, Lin J, Chen P (2020) An evoluted bio-based 2,5-furandicarboxylate copolyester fiber from poly(ethylene terephthalate). J Polym Sci 58:320–329

[25] Pan J, Zhang D, Wu M, Ruan S, Castro JM, James Lee L, Chen F (2020) Impacts of carbonaceous particulates on extrudate semicrystalline polyethylene terephthalate foams: nonisothermal crystallization, rheology, and infrared attenuation studies. Ind Eng Chem Res 59:15586–15597

[26] Jiang C, Han S, Chen S, Zhou H, Wang X (2020) Crystallization-induced microcellular foaming behaviors of chain-extended polyethylene terephthalate. Cell Polym 39:223–237

[27] Yang Z, Xin C, Mughal W, Li X, He Y (2018) High-melt-elasticity poly(ethylene terephthalate) produced by reactive extrusion with a multi-functional epoxide for foaming. J Appl Polym Sci 135:45805

[28] Ge Y, Yao S, Xu M, Gao L, Fang Z, Zhao L, Liu T (2019) Improvement of poly(ethylene terephthalate) melt-foamability by long-chain branching with the combination of pyromellitic dianhydride and triglycidyl isocyanurate. Ind Eng Chem Res 58:3666–3678

[29] Yan H, Yuan H, Gao F, Zhao L, Liu T (2015) Modification of poly(ethylene terephthalate) by combination of reactive extrusion and followed solid-state polycondensation for melt foaming. J Appl Polym Sci 132:42708

[30] Jiang C, Han S, Chen S, Zhou H, Wang X (2021) The role of PTFE in-situ fibrillation on PET microcellular foaming. Polymer 212:123171

[31] Li D, Liu T, Zhao L, Yuan W (2012) Controlling sandwich-structure of PET microcellular foams using coupling of CO_2 diffusion and induced crystallization. AIChE J 58:2512–2523

[32] Xia T, Xi Z, Liu T, Zhao L (2017) Solid state foaming of poly(ethylene terephthalate) based on periodical CO_2-renewing sorption process. Chem Eng Sci 168:124–136

[33] Wang Z, Wang J, Pang Y, Zhu J, Zheng W (2022) Dependence of the foaming window of poly(ethylene terephthalate-co-ethylene 2,5-furandicarboxylate) copolyesters on FDCA content. Polymer 254:125101

[34] Guo B, Pang Y, Cao X, Chen Q, Zheng W (2020) A creative approach to prepare structure-tunable multilayered PMMA/PS/PMMA foams. Polymer 209:123061

[35] Pang Y, Cao Y, Guo B, Zhou H, Fang W, Xi J, Liu X, Zhou Y, Weng Y, Zheng W (2021) Unprecedented cell structure variation in multilayered alternating $PS/PS-SiO_2$ foams. ACS Appl Polym Mater 3:2687–2693

[36] Pang Y, Zhang X, Guo B, Wang Z, Fang W, Li J, Zheng W (2021) Unprecedented cell structure variation in multilayered alternating PS/PMMA foams. Polymer 237:124386

[37] Wang K, Wang S, Wu F, Pang Y, Liu W, Zhai W, Zheng W (2016) A new strategy for preparation of long-chain branched polypropylene via reactive extrusion with supercritical CO_2 designed for an improved foaming approach. J Mater Sci 51:2705–2715 https://doi.org/10.1007/s10853-015-9584-x

[38] Cao Y, Pang Y, Dong X, Wang D, Zheng W (2021) To clarify the resilience of PEBA/MWCNT foams via revealing

the effect of the nanoparticle and the cellular structure. ACS Appl Polym Mater 3:3766–3775

[39] Liu H, Ma J, Gong J, Xu J (2015) The effect of Pglass state on the non-isothermal cold and melt crystallization processes of PET matrix. Thermochim Acta 613:1–8

[40] Han Z, Wang Y, Wang J, Wang S, Zhuang H, Liu J, Huang L, Wang Y, Wang W, Belfiore LA, Tang J (2018) Preparation of hybrid nanoparticle nucleating agents and their effects on the crystallization behavior of poly(ethylene terephthalate). Materials 11:587

[41] Doroudianl S, Park CB, Kortschot MT (1996) Effect of the crystallinity and morphology on the microcellular foam structure of semicrystalline polymers. Polym Eng Sci 36:2645–2661

[42] Wan C, Lu Y, Liu T, Zhao L, Yuan W (2017) Foaming of low density polyethylene with carbon dioxide based on its in situ crystallization behavior characterized by high-pressure rheometer. Ind Eng Chem Res 56:10702–10710

[43] Cao Y, Pang Y, Dong X, Wang D, Zheng W (2020) Cell structure variation in poly(ether-mb-amide) copolymer foams induced by chemi-crystallization. Ind Eng Chem Res 59:11340–11349

[44] Wu D, Cheng Y, Feng S, Yao Z, Zhang M (2013) Crystallization behavior of polylactide/graphene composites. Ind Eng Chem Re 52:6731–6739

[45] Bussiere PO, Therias S, Gardette JL, Murariu M, Dubois P, Baba M (2012) Effect of ZnO nanofillers treated with tri-ethoxy caprylylsilane on the isothermal and non-isothermal crystallization of poly(lactic acid). Phys Chem Chem Phys 14:12301–12308

[46] Chen P, Wang W, Wang Y, Yu K, Zhou H, Wang X, Mi J (2017) Crystallization-induced microcellular foaming of poly(lactic acid) with high volume expansion ratio. Polym Degrad Stabil 144:231–240

[47] Ni J, Yu K, Zhou H, Mi J, Chen S, Wang X (2020) Morphological evolution of PLA foam from microcellular to nanocellular induced by cold crystallization assisted by supercritical CO_2. J Supercrit Fluid 158:104719

[48] Li B, Zhao G, Wang G, Zhang L, Hou J, Gong J (2019) A green strategy to regulate cellular structure and crystallization of poly(lactic acid) foams based on pre-isothermal cold crystallization and CO_2 foaming. Int J Biol Macromol 129:171–180

[49] Li B, Zhao G, Wang G, Zhang L, Gong J (2018) Fabrication of high-expansion microcellular PLA foams based on pre-isothermal cold crystallization and supercritical CO_2 foaming. Polym Degrad Stabil 156:75–88

[50] Pang Y, Cao Y, Zheng W, Park CB (2022) A comprehensive review of cell structure variation and general rules for polymer microcellular foams. Chem Eng J 430:132662

[51] Zheng W, Lee YH, Park CB (2010) Use of nanoparticles for improving the foaming behaviors of linear pp. J Appl Polym Sci 117:2972–2979

[52] Ji G, Zhai W, Lin D, Ren Q, Zheng W, Jung DW (2013) Microcellular foaming of poly(lactic acid)/silica nanocomposites in compressed CO_2: critical influence of crystallite size on cell morphology and foam expansion. Ind Eng Chem Res 52:6390–6398

[53] Wang L, He Y, Jiang T, Zhang X, Zhang C, Peng X (2019) Morphologies and properties of epoxy/multi-walled carbon nanotube nanocomposite foams prepared through the free-foaming and limited-foaming process. Compos Sci Technol 182:107776

[54] Wang G, Zhao J, Wang G, Mark LH, Park CB, Zhao G (2017) Low-density and structure-tunable microcellular PMMA foams with improved thermal-insulation and compressive mechanical properties. Eur Polym J 95:382–393

[55] Shi Z, Zhao G, Zhang L, Wang G, Chai J (2022) Ultralight and hydrophobic PVDF/PMMA open-cell foams with outstanding heat-insulation and oil-adsorption performances fabricated by CO_2 molten foaming. J CO_2 Util 63: 102108